

D-TRANSFORM BASED CONTROL OF POWER CONVERTERS

A. H. R. Rosa¹, W. W. A. G. Silva², W. he³, F. A. da Silva¹, L. M. F. Morais⁴, S. I. Seleme Jr.⁴

¹Instituto Federal de Minas Gerais - Campus Betim - Betim, MG - Brasil,

²Universidade Federal de Itajubá - UNIFEI, MG - Brasil.

³School of Automation, Nanjing University of Information Science and Technology, China,

⁴Universidade Federal de Minas Gerais, MG - Brasil.

e-mail: arthurhrosa@gmail.com

Abstract – The aim of this study is to present a very simple, intuitive and feasible tool: the D-transform between converters. This new method proposes to find a control equation of any pre-defined control law from one converter to another power converter. The central goal is to take maximum advantage of the robustness offered by the originator nonlinear control law. Although there is the possibility of more than one conversion, some candidates show good performance in terms of transient overshoot, settling time and steady-state regulation. The stability proof is disposed individually for each generated equation. The performance of D-Controllers is verified through Hardware In the Loop (HIL) simulations. A small overshoot under input and load perturbations is achieved for the buck-boost example. Finally, a experimental validation using a buck converter is given to illustrate the application method and the nonlinear control design.

Keywords – D-Transform, buck, buck-boost, boost, SFL, IDAPBC, relations, HIL Simulation, nonlinear control.

NOMENCLATURE

E	Input voltage.
μ	Generalized duty cycle.
U	Steady-State duty cycle.
D	Boost duty cycle.
d	Buck duty cycle.
δ	Buck-boost duty cycle.
x_1	Inductor current.
x_2	Capacitor voltage.
V_d	Desired output voltage.
x_{2d}	Output voltage reference.
L	Converters inductance.
C	Converters capacitance.
G	Load conductance.
R	Load resistance.
x'	Complementer operator (1-x).
\bar{x}	Steady-state value.
k_1	SFL gain controller.
k_α	CIDAPBC gain controller.
k_z	IDAPBC gain controller.

I. INTRODUCTION

The design of non-conventional methods for solving power electronics and control problems is an emerging area [1], [2]. There are many reasons to use non-classical techniques, such as energy savings, cost reductions and, obviously, the increase of dynamic performance, large stability margin, and high robustness [3], [4], [5]. Therefore, this paper presents a new perspective regarding the control of static power converters that play a key role in several emerging applications including power systems [6], transformers [7], dc micro-grids [8] - [9], electric vehicles and aircrafts [10] - [11], integrated energy systems [12], photovoltaic systems [13] 1, cyber-physical systems [2], inverters [14], etc ...

Through the employment of average nonlinear dynamic model, different nonlinear control methods have been addressed to regulate the desired voltage or current and achieve the stability of the closed-loop system [15]. Nonlinear controllers have been successfully applied to dc/dc converters established by a rigorous mathematical formulation, and are, in many cases, combined with the traditional PI control [16]. Nevertheless, almost all of the existing control methods for dc/dc converters requisite exact knowledge of the converter parameters (capacitance, inductance) or the load impedance to assure nonlinear stability.

The Laplace, Fourier and Z-transforms [17] are remarkable tools in different domains, e.g., control, signal processing, telecommunications and electronic engineering. The central purpose is to directly apply the preferred and simplified equations that can be used in several practical applications. Inspired by this motion, we aim at designing a transform function of converter equations. To be specific, this work outlines a methodology to achieve nonlinear control based on D-Transform, which will be better described in dedicated section.

The first reason is the rapid generation of control equations extended of one converter to another. The second motivation is to produce a new family of controllers based on previously developed equations that will be redesigned. Such new control laws meet the requirements for new insights and robustness criteria of advanced controllers.

What is the D-Transform ? By definition, the D-transform is comprised of finding, straightly, a function that converts an equation of the duty cycle μ from one converter to another converter, through the existing input to output relations of

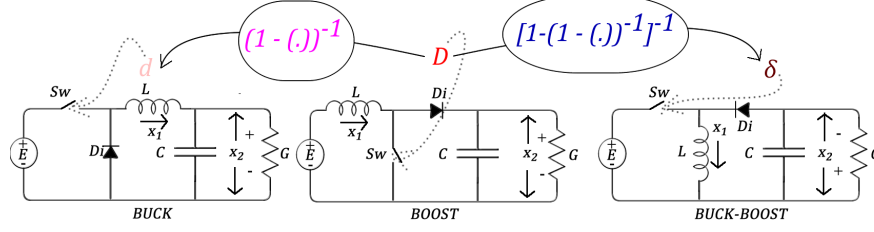


Fig. 1. Typical power converters and proposed D-Transform. Buck duty cycle (d), Boost duty cycle (D), and Buck-boost duty cycle (δ).

TABLE I
Converters models

	Boost	Buck	Buck-Boost
SSM	$\dot{x}_1 = -(1-\mu)\frac{1}{L}x_2 + \frac{E}{L}$ $\dot{x}_2 = (1-\mu)\frac{1}{C}x_1 - \frac{G}{C}x_2$	$\dot{x}_1 = -\frac{1}{L}x_2 + \mu\frac{E}{L}$ $\dot{x}_2 = \frac{1}{C}x_1 - \frac{G}{C}x_2$	$\dot{x}_1 = (1-\mu)\frac{1}{L}x_2 + \mu\frac{E}{L}$ $\dot{x}_2 = -(1-\mu)\frac{1}{C}x_1 - \frac{G}{C}x_2$
SSM_n^{0*}	$\dot{x}_{1n} = -\mu'x_{2n} + 1$ $\dot{x}_{2n} = \mu x_{1n} - \frac{1}{Q}x_{2n}$	$\dot{x}_{1n} = -x_{2n} + \mu$ $\dot{x}_{2n} = x_{1n} - \frac{1}{Q}x_{2n}$	$\dot{x}_{1n} = \mu'x_{2n} + \mu$ $\dot{x}_{2n} = -\mu'x_{1n} - \frac{1}{Q}x_{2n}$
ELM	$D_B\dot{x} + (1-\mu)J_{Bx} + R_Bx = F$ $J_B = \begin{bmatrix} 0 & 1 \\ -1 & 0 \end{bmatrix};$ $x = \begin{bmatrix} x_1 \\ x_2 \end{bmatrix}; D_B = \begin{bmatrix} L & 0 \\ 0 & C \end{bmatrix}; R_B = \begin{bmatrix} 0 & 0 \\ 0 & G \end{bmatrix}; F = \begin{bmatrix} E \\ 0 \end{bmatrix}$	$D_B\dot{x} + (J_B + R_B)x = \mu F$ $J_B = \begin{bmatrix} 0 & 1 \\ -1 & 0 \end{bmatrix}$ $x = \begin{bmatrix} x_1 \\ x_2 \end{bmatrix}; D_B = \begin{bmatrix} L & 0 \\ 0 & C \end{bmatrix}; R_B = \begin{bmatrix} 0 & 0 \\ 0 & G \end{bmatrix}; F = \begin{bmatrix} E \\ 0 \end{bmatrix}$	$D_B\dot{x} + (1-\mu)J_{Bx} + R_Bx = \mu F$ $J_B = \begin{bmatrix} 0 & -1 \\ 1 & 0 \end{bmatrix};$ $x = \begin{bmatrix} x_1 \\ x_2 \end{bmatrix}; D_B = \begin{bmatrix} L & 0 \\ 0 & C \end{bmatrix}; R_B = \begin{bmatrix} 0 & 0 \\ 0 & G \end{bmatrix}; F = \begin{bmatrix} E \\ 0 \end{bmatrix}$
PHC	$J_H = \begin{bmatrix} 0 & -\frac{1-\mu}{LC} \\ \frac{1-\mu}{LC} & 0 \end{bmatrix};$ $R_H = \begin{bmatrix} 0 & 0 \\ 0 & \frac{1}{RC^2} \end{bmatrix}; g_H = \begin{bmatrix} \frac{1}{L} \\ 0 \end{bmatrix}$ $x = \begin{bmatrix} x_1 \\ x_2 \end{bmatrix}; \dot{x} = [J_H(\mu) - R_H] \frac{\partial H}{\partial x}(x) + g_H E; H(x) = \frac{1}{2}Lx_1^2 + \frac{1}{2}Cx_2^2$	$J_H = \begin{bmatrix} 0 & -\frac{1}{LC} \\ \frac{1}{LC} & 0 \end{bmatrix};$ $R_H = \begin{bmatrix} 0 & 0 \\ 0 & \frac{1}{RC^2} \end{bmatrix}; g_H = \begin{bmatrix} \frac{\mu}{L} \\ 0 \end{bmatrix}$ $x = \begin{bmatrix} x_1 \\ x_2 \end{bmatrix}; \dot{x} = [J_H(\mu) - R_H] \frac{\partial H}{\partial x}(x) + g_H E; H(x) = \frac{1}{2}Lx_1^2 + \frac{1}{2}Cx_2^2$	$J_H = \begin{bmatrix} 0 & \frac{1-\mu}{LC} \\ -\frac{1-\mu}{LC} & 0 \end{bmatrix};$ $R_H = \begin{bmatrix} 0 & 0 \\ 0 & -\frac{1}{RC^2} \end{bmatrix}; g_H = \begin{bmatrix} \frac{\mu}{L} \\ 0 \end{bmatrix}$ $x = \begin{bmatrix} x_1 \\ x_2 \end{bmatrix}; \dot{x} = [J_H(\mu) - R_H] \frac{\partial H}{\partial x}(x) + g_H E; H(x) = \frac{1}{2}Lx_1^2 + \frac{1}{2}Cx_2^2$

these converters, which are functions of the duty-cycle.

Moreover, the control methods used in this work are the State Feedback Linearization (SFL) [18] - [19], Interconnection and Damping Assignment Passivity-Based Control (IDA-PBC) [20] and other nonlinear control equations derived via D-Transform, whose models and control formulations are demonstrated in section II. The proposed D-Transform approach is explained in section III. Finally, results and conclusions are presented in section IV and V.

II. MODELING AND RELATIONS BETWEEN CONVERTERS

The basic dc-dc power converters - as boost, buck, and buck-boost shown in Figure 1 - are typical building blocks in power electronics, that have the same elements: one diode, one switch, one capacitor and one inductor. The difference between them comprises the physical position of such elements. Furthermore, the nonlinear behaviour is mainly present on semiconductor components (diode and switch).

Table I condenses three distinct models commonly found in the literature: Euler-Lagrange Model (ELM), State-Space Model (SSM) and Port-Controlled Hamiltonian (PCH). It should be emphasized that the Euler-Lagrange approach presents an equivalent form of buck-boost and boost modelling. In sequence, PCH model evidences a similar structure for the three converters. Possible problems encountered in boost and buck-boost converters are related to the occurrence of right-half-plane (RHP) zeros, which troublesome characteristic brings to nonminimum-phase [21].

Additionally, RHP zero is the origin of bandwidth limitation and instability of closed-loop system [22].

A. Equilibrium's relation of power converters

The relations addressed in the following sentences - and summarized in Table II - are reported by the majority of power electronics book. Even so, we replicate some essential relations that will be employed to attain the proposed D-transform. It can be noted that these relations are for the ideal DC-DC converters in CCM (Continuous Current Mode) operation.

Boost

The circuit of boost converter circuit can be modelled by average space state equations:

$$\dot{x}_1 = -(1-D)\frac{1}{L}x_2 + \frac{E}{L}; \dot{x}_2 = (1-D)\frac{1}{C}x_1 - \frac{G}{C}x_2. \quad (1)$$

where x_1 denotes the inductor current, x_2 is the capacitor voltage, E is the input voltage, x_n is the normalized state variable.

In the steady state, by substituting $\dot{x}_1 = 0$ and $\dot{x}_2 = 0$ in (1), the equilibrium points of the boost converter are given by:

$$\bar{x}_1 = \frac{EG}{(1-D)^2}, \bar{x}_2 = \frac{E}{(1-D)}. \quad (2)$$

normalized models are obtained by considering [23] : $\tau = \frac{1}{\sqrt{LC}}, x_{1n} = \frac{1}{E}\sqrt{\frac{L}{C}}x_1, x_{2n} = \frac{1}{E}x_2, \dot{x}_{1n} = \frac{\dot{x}_1}{\tau}$

TABLE II
Relation equations

	SFL control equation	Open loop ($U = \bar{d}, \bar{D}, \bar{\delta}$)		Slew rate	$\frac{V_d}{E}$	Transformation
Buck	$d = \frac{-k_1(x_1 - x_{1d}) + x_2}{E}$	$\bar{d} = 1 - \frac{E - V_d}{E}$	$\bar{d} = \frac{V_d}{E}$	$\bar{d}' = 1 - \bar{d} = \frac{E - V_d}{E}$	μ	$d = (D')^{-1}$
Boost	$D = 1 - \frac{[E + k_1(x_1 - x_{1d})]x_2}{x_2 - E}$	$\bar{D} = 1 - \frac{E}{V_d}$	$\bar{D} = \frac{V_d - E}{V_d}$	$\bar{D}' = 1 - \bar{D} = \frac{E}{V_d}$	$\frac{1}{(1-\mu)}$	$\frac{1}{(1-D)}$
Buck-Boost	$\bar{\delta} = \frac{+k_1(x_1 - x_{1d}) + x_2}{x_2 - E}$	$\bar{\delta} = 1 - \frac{E}{E - V_d}$	$\bar{\delta} = \frac{V_d}{E - V_d}$	$\bar{\delta}' = 1 - \bar{\delta} = \frac{E}{E - V_d}$	$-\frac{\mu}{(1-\mu)}$	$-\frac{\delta}{(1-\delta)}$

TABLE III
Transfer functions (found in [24])

Converter	G_{R0}	G_{d0}	w_0	Q	w_z
Buck	U	$\frac{V_d}{U}$	$\frac{1}{\sqrt{LC}}$	$R\sqrt{\frac{C}{L}}$	∞
Boost	$\frac{1}{U'}$	$\frac{V_d}{U'}$	$\frac{U'}{\sqrt{LC}}$	$U'R\sqrt{\frac{C}{L}}$	$\frac{U'2R}{L}$
Buck-boost	$\frac{-U}{U'}$	$\frac{V_d}{U'}$	$\frac{U'}{\sqrt{LC}}$	$U'R\sqrt{\frac{C}{L}}$	$\frac{U'2R}{UL}$

By considering \bar{D} as a constant control input in view of (2), one gets:

$$\bar{x}_1 = \frac{G}{E} \bar{x}_2^2. \quad (3)$$

Now, replacing the desired output capacitor voltage as $\bar{x}_2 = V_d$, the equilibrium points \bar{x} and the fixed input control \bar{D} are given by:

$$\bar{D} = 1 - \frac{E}{V_d}, \bar{x} = [\bar{x}_1, \bar{x}_2]^T = \left[GV_d \left(\frac{V_d}{E} \right), V_d \right]^T. \quad (4)$$

Buck

Next let us consider the buck converter, some simple calculations show that:

$$\bar{x}_1 = dEG, \bar{x}_2 = dE, \bar{x}_1 = G\bar{x}_2, \bar{d} = 1 - \frac{E - V_d}{E}, \quad (5)$$

$$\bar{x} = [\bar{x}_1, \bar{x}_2]^T = [GV_d, V_d]^T.$$

The State-Space Modelling of step down converter is given by:

$$\dot{x}_1 = -\frac{1}{L}x_2 + d\frac{E}{L}, \quad (6)$$

$$\dot{x}_2 = \frac{1}{C}x_1 - \frac{G}{C}x_2, \quad (7)$$

The equilibrium points of buck converter is obtained when replacing $\dot{x} = 0$ in (6)-(7) :

$$\bar{x}_1 = dEG, \quad (8)$$

$$\bar{x}_2 = dE. \quad (9)$$

By considering d as a fixed value in (8)-(9) leads to:

$$\bar{x}_1 = G\bar{x}_2. \quad (10)$$

Therefore, the fixed open loop control \bar{d} to stabilize \bar{x} is:

$$\bar{d} = 1 - \frac{E - V_d}{E}, \quad (11)$$

$$\bar{x} = [\bar{x}_1, \bar{x}_2]^T = [GV_d, V_d]^T.$$

Buck-boost

The equivalent SSM of buck-boost can be expressed in the following form:

$$\dot{x}_1 = (1 - \delta) \frac{1}{L} x_2 + \delta \frac{E}{L}, \quad (12)$$

$$\dot{x}_2 = -(1 - \delta) \frac{1}{C} x_1 - \frac{G}{C} x_2, \quad (13)$$

When substituting $\dot{x}_1 = 0$ and $\dot{x}_2 = 0$ in (12)-(13), one obtains:

$$\bar{x}_1 = \frac{\delta EG}{(1 - \delta)^2}. \quad (14)$$

$$\bar{x}_2 = -\frac{\delta E}{(1 - \delta)}. \quad (15)$$

By replacing $\bar{\delta}$ in (14)-(15), we have:

$$\bar{x}_1 = G\bar{x}_2 \left(\frac{\bar{x}_2}{E} - 1 \right). \quad (16)$$

Thus, the equilibrium points to stabilize \bar{x} and the constant input control $\bar{\delta}$ given by:

$$\bar{\delta} = 1 - \frac{E}{E - V_d}, \quad (17)$$

$$\bar{x} = [\bar{x}_1, \bar{x}_2]^T = \left[GV_d \left(\frac{V_d}{E} - 1 \right), V_d \right]^T.$$

So, the summarized equations for buck-boost converter are:

$$\bar{x}_1 = \frac{\delta EG}{(1 - \delta)^2}, \bar{x}_2 = -\frac{\delta E}{(1 - \delta)}, \bar{x}_1 = G\bar{x}_2 \left(\frac{\bar{x}_2}{E} - 1 \right),$$

$$\bar{\delta} = 1 - \frac{E}{E - V_d}, \bar{x} = [\bar{x}_1, \bar{x}_2]^T = \left[GV_d \left(\frac{V_d}{E} - 1 \right), V_d \right]^T. \quad (18)$$

B. Transfer Functions of linearized models

Table III exhibits parameters of both control-to-output (G_{vd}) and input-to-output (G_{vi}) transfer functions of the basic

TABLE IV
Canonical Circuit Parameter (Found in [24])

Converter	$M(U)$	L_c	$e(s)$	$j(s)$
Buck	U	L	$\frac{V_d}{U^2}$	$\frac{V_d}{R}$
Boost	$\frac{1}{U'}$	$\frac{L}{U'^2}$	$V_d \left(1 - \frac{sL}{U'^2 R}\right)$	$\frac{V_d}{U'^2 R}$
Buck-boost	$\frac{-U}{U'}$	$\frac{L}{U'^2}$	$\frac{-V_d}{U'^2} \left(1 - \frac{sL}{U'^2 R}\right)$	$\frac{-V_d}{U'^2 R}$

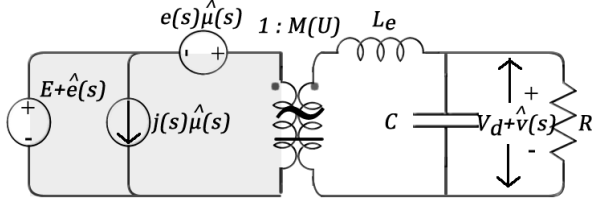


Fig. 2. Canonical power converters circuits.

boost, buck and buck-boost converters [24]:

$$G_{vi}(s) = G_{i0} \frac{1}{1 + \frac{s}{Q\omega_0} + \left(\frac{s}{\omega_0}\right)^2}, \quad (19)$$

$$G_{vd}(s) = G_{d0} \frac{\left(1 - \frac{s}{\omega_z}\right)}{\left(1 + \frac{s}{Q\omega_0} + \left(\frac{s}{\omega_0}\right)^2\right)}. \quad (20)$$

The canonical form of converters is shown in Figure 2. The straight derivation of the transfer functions is displayed in Table IV. All tables presented in this work make an effort to clarify common characteristics among the converts, so they are customized as potential sources of D-candidates.

III. MAIN IDEA : THE D-TRANSFORM

Figure 3 shows the flowchart of the proposed methodology. The D-Transform design proceeds in following steps:

1. Converter: choose a converter as a starting point. In this work, the boost was selected.
2. Inputs : it is possible to apply any nonlinear control based equations. We use SFL and IDAPBC control laws, for example.
3. D-Transform: the next step is to apply the D-transform, firstly, by considering intuitive relations (e.g.: steady-state equations), and then nontrivial relations.
4. Outputs: the new D-Controllers (e.g.: D-SFL, D-CIDAPBC, D-IDAPBC).
5. Validation: finally, the new generated control equations can be verified by software simulations, stability analysis and hardware tests.

Definition 1. *The D-transform consists of finding, directly, a function that establishes the duty cycle μ from one converter to another.*

Surrounded by several candidates, we choose as initial point the following transformation equations:

Proposition 1. *There is a transformation function Δ_1 that*

converts $D \rightarrow d, \delta$:

$$d, \delta = \Delta_1(D), d = (D')^{-1}, \delta = 1 - [1 - (D')^{-1}]^{-1}. \quad (21)$$

Example 1. *The root of Δ_1 is related to steady-state investigation. To simplify the notation, let us replicate the buck and boost equations given by (4)-(5):*

$$\bar{D} = \frac{V_d - E}{V_d}, \bar{d} = \frac{V_d}{E}. \quad (22)$$

It is possible to define a expression that leads $\bar{D} \Rightarrow \bar{d}$ (consequently, $D \Rightarrow d$). It should be noted that the equation conversion is given by (21) and the second column of Table III.

Proposition 2. *There exist other transformation functions $\Delta_2, \Delta_3, \dots, \Delta_n$ that convert $D \rightarrow \delta$:*

$$\delta = \Delta_2(D), \delta = -\frac{D^{-1}}{D'} \quad (23)$$

$$\delta = \Delta_3(D), \delta = 1 + D'. \quad (24)$$

Example 2. *Let us repeat the control gain G_{i0} of Table III:*

$$G_{i0} = \frac{-U}{U'}, \quad (25)$$

By replacing U - generalized duty cycle in steady-state - by D it is important to recall that (23) and (25) are similar.

To investigate the applications of D-transform we choose recently nonlinear equations found in the literature. For simplicity, we use two control laws based on IDAPBC. In [25], Classic IDAPBC (referenced as CIDAPBC) is addressed to boost converters achieving a simple control equation described by: *CIDAPBC*:

$$\bar{D} = 1 - \frac{E}{V_d}, D = 1 - (1 - \bar{D}) \left(\frac{x_2}{V_d}\right)^{k_\alpha}. \quad (26)$$

In addition, [20] modify and improve (26) to obtain: *IDAPBC*:

$$D = 1 - \frac{k_z E}{2Ex_2 + (k_z - 2E)x_{2d}}. \quad (27)$$

For didactic purposes, we also add the nonlinear SFL equation [15]:

$$D = 1 - \frac{[E + k_1(x_1 - x_{1d})]}{x_2}. \quad (28)$$

By replacing the results of (26)-(28) in (21)-(24), we collect the new D-equations gathered in Table II (where k_1, k_α and k_z are the nonlinear control gains).

Example 3. *So, the new D-SFL control equation is performed by evaluation of (21) and (28):*

$$d = \frac{x_2}{[E + k_1(x_1 - x_{1d})]}. \quad (29)$$

TABLE V
D-Transform Control equations

	SFL	D-SFL		IDAPBC	D-IDAPBC
Buck	$d = \frac{-k_1(x_1 - x_{1d}) + x_2}{E}$	$d = \frac{x_2}{E + k_1(x_1 - x_{1d})}$	← Eq.(21) →	→ → → → → → → →	$d = \frac{2Ex_2 + (k-2E)x_{2d}}{kE}$
Boost (source)	$D = 1 - \frac{[E + k_1(x_1 - x_{1d})]}{x_2}$	-		$D' = \frac{kE}{2Ex_2 + (k-2E)x_{2d}}$	-
Buck- Boost	$\delta = \frac{+k_1(x_1 - x_{1d}) + x_2}{x_2 - E}$	$\delta = \frac{-x_2}{k_1(x_1 - x_{1d}) + E - x_2}$	← Eq.(21)	Eq.(24) → → → → →	$\delta = 1 + \frac{kE}{2Ex_2 + (k-2E)x_{2d}}$

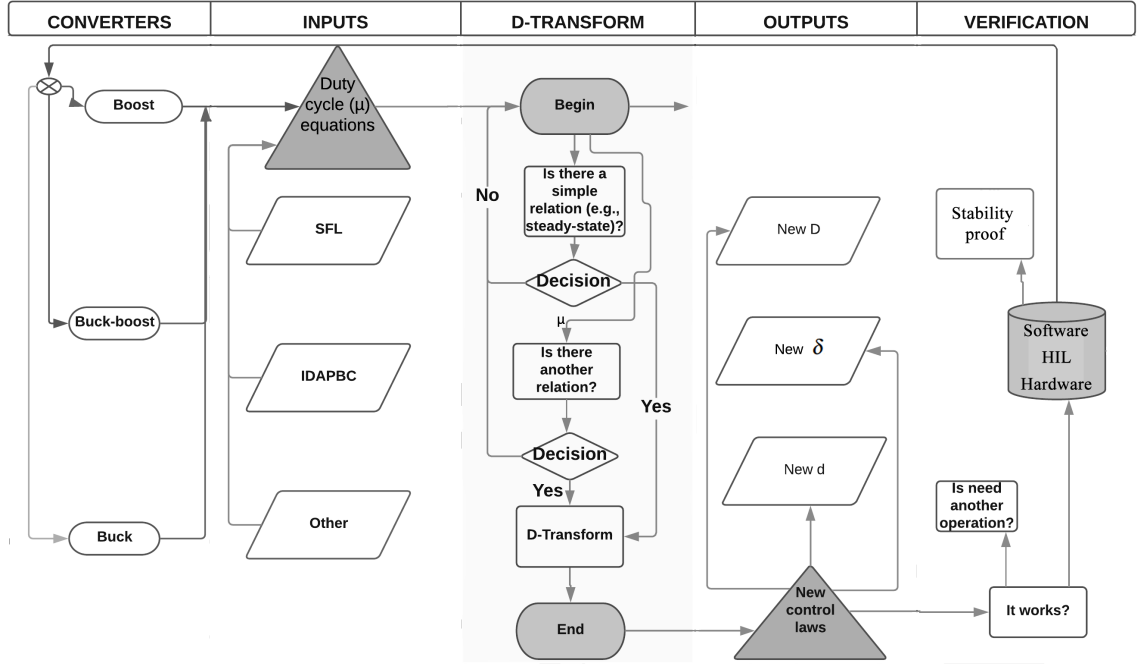


Fig. 3. Flowchart of D-Transform.

TABLE VI
D-Transform Control equations

	CIDAPBC	D-CIDAPBC
Buck	-	$d = 1 - (1 - \bar{d}) \left(\frac{x_2}{\bar{v}_d} \right)^{-k\alpha}$
Boost	$D = 1 - (1 - \bar{D}) \left(\frac{x_2}{\bar{v}_d} \right)^{k\alpha}$	
Buck- Boost	-	$\delta = 1 - (1 - \bar{\delta}) \left(\frac{x_2}{\bar{v}_d} \right)^{k\alpha}$

Example 4. By substituting (27) in (24):

$$\delta = 1 + \frac{k_z E}{2Ex_2 + (k_z - 2E)x_{2d}}. \quad (30)$$

A. Stability analyses

Two main goals are to be analyzed, regarding the stability of the closed-loop system: (i) the equilibrium of the system and (ii) the zero dynamics at the equilibrium. The control design consists in, first, rendering the error $(x - x_d)$ equal to zero, and, there, ensuring asymptotic stability to the error dynamics. As proved by [26], the system is asymptotically stable if the new control law is satisfied and the ‘zero dynamics’ around the

desired equilibrium point are stable. In order to evaluate the stability of the internal dynamics of the closed loop system, the standard approach is to consider the corresponding zero dynamics. As long as the zero dynamics is asymptotically stable, the internal dynamics will be locally exponentially stable [27]. Thus, the equation describing the zero-order dynamics is obtained by making the error equal to zero and replacing the state variables by their respective steady-state values.

Example 5. The zero-order dynamics of the D-SFL buck control equation is obtained by using terms of (5) and (29):

$$\bar{\mu} = \frac{x_{20}}{E}, \quad (31)$$

$$\dot{x}_{20} = \frac{\bar{x}_1 - G\bar{x}_2}{C}. \quad (32)$$

As $\bar{x}_2 = \bar{\mu}E$ and $\bar{d} = \bar{\mu}$ for the buck converter, deriving the two sides of (31) and substituting in (32), the zero order dynamics as a function of $\bar{\mu}$:

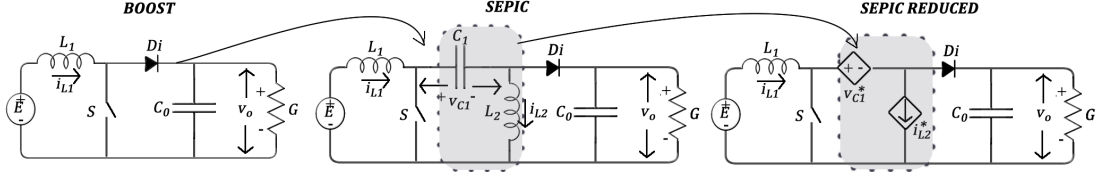


Fig. 4. Reduced SEPIC

$$\dot{\bar{\mu}} = \frac{G}{C} \left(\bar{\mu} - \frac{\bar{x}_1}{GE} \right) \quad (33)$$

which the equilibrium point, $\bar{\mu} = \frac{\bar{x}_1}{GE}$, is stable (similar procedure is obtained in [26] and [28]).

B. d -Transform and δ -Transform

We choose the boost as base converter to generate D-Controllers for buck and buck-boost converters. However, the same strategy can be applied to attain the new D control laws from the buck (d -Transform) and also from the buck-boost (δ -Transform). In other to clarify this suggestion, the evaluation of $d \rightarrow \delta$ is given by:

$$\delta = 1 - (d')^{-1}. \quad (34)$$

The D-Controllers achieved for the buck-boost can be adapted to flyback converter, which is widely used in cellular power supplies and in other applications like LED and solar power system, for example [29]. For generation equations from buck to boost converter:

$$D = (d^{-1})'. \quad (35)$$

Example 6. Let us replicate the buck and boost equations given by (4)-(5):

$$\bar{D} = \frac{V_d - E}{V_d}, \bar{d} = \frac{V_d}{E}. \quad (36)$$

It is possible to define a expression that leads $\bar{d} \Rightarrow \bar{D}$ (consequently, $d \Rightarrow D$). It should be noted that the equation conversion is given by (35).

C. Extension to other converters

Figure 4 shows the boost and SEPIC converters for comparison. It can be noted that when removing the intermediate elements (L_2, C_1) highlighted by the dotted line, the SEPIC converter becomes similar to the boost converter, having similar equilibrium points as shown in Table VII.

Therefore, we can use the boost equations and apply them to control the SEPIC converter replacing the eliminated state variables (i_{L2} and v_{c1}) by the equilibrium points, provided in

TABLE VII
Equilibrium points of the converters.

Converter	i_{L1}^*	v_o^*	i_{L2}^*	v_{c1}^*
Boost	$\frac{G}{E} V_d^2$	V_d	-	-
SEPIC	$\frac{G}{E} V_d^2$	V_d	GV_d	E

Table VII, represented by dependent sources in the model. If we substitute, for example, v_{c1} by E and i_{L2} by GV_d in the SEPIC converter, it saves two sensors. Figure 4 summarizes this process. So the equation to transform the boost duty cycle D to SEPIC duty cycle D_s is:

$$D = D_s. \quad (37)$$

For CUK converter, Equation (37) can be applied as reported in [30].

D. The integral action

The transformations, the nonlinear models and control equations require accurate knowledge of the converter parameters. Thus, in order to constrain the voltage output to get the desired value V_d , it is useful to include a proportional integrative (PI) term in the control equation, given by [31], [32]:

$$G_{int} = -k_{int} \int_0^t [x_2(s) - V_d] ds. \quad (38)$$

Equation (38) can be applied for all converters using D-Controllers, IDAPBC, SFL or other nonlinear control law. For example, by considering the D-SFL control and the buck converter:

$$d = \frac{x_{2d}}{[E + k_1(x_1 - x_{1d})]}, \quad (39)$$

$$x_{2d} = -k_{int} \int_0^t [x_2(s) - V_d] ds.$$

IV. SOFTWARE SIMULATION AND HIL RESULTS

Simulations are made to compare the performance of D-Controllers using Matlab/Simulink and Single Hardware in The Loop (SHIL) approach [33]. In all simulations, we have chosen the system parameters and design specifications shown in Table 7 and the D-control laws (Tables V and VI).

In Figure 5-B we present the transient responses of the output voltage of the buck-boost under load perturbation, by considering original SFL and derived D-SFL, D-IDAPBC and D-CIDAPBC control methods. The same scheme is shown in Figure 5-C for the buck converter. In these simulations, consecutive load step variation of 70% to 100% are applied. Figure 5-A, D shows the output capacitor voltage x_2 using Hardware in the loop. Figure 6 reveals the input variation tests.

As seen in Figure 4 and 5, both software simulations and HIL results reach the steady state value after the step variation. It is remarkable that the performance of the systems are in agreement, since the same transient dynamics is observed,

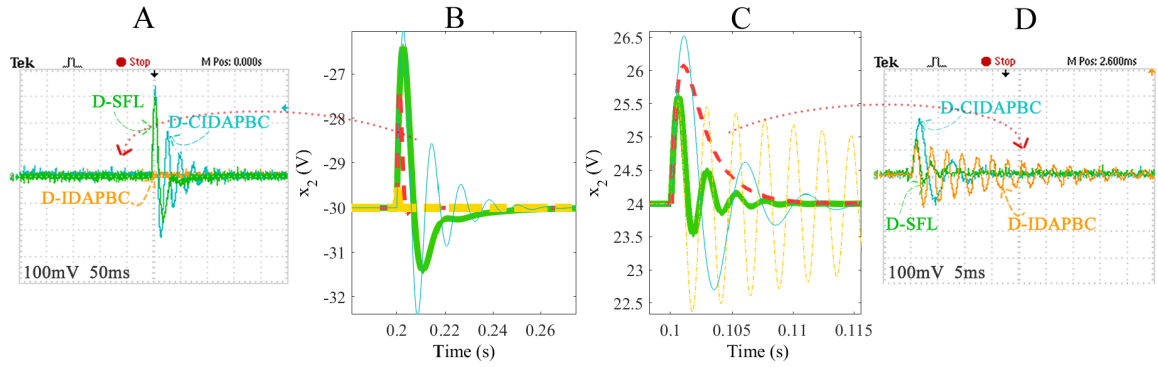


Fig. 5. Software simulation result (Matlab/Simulink) using control techniques SFL (dashed red), D-SFL (continue green) D-CICAPBC (continue cyan), D-IDAPBC (dashed yellow). Output voltage x_2 for buck-boost (B) and buck (C) in view of load variation (70-100 %) in 0.1s and 0.2s. HIL experimental result, normalized output voltage x_2 (A-D).

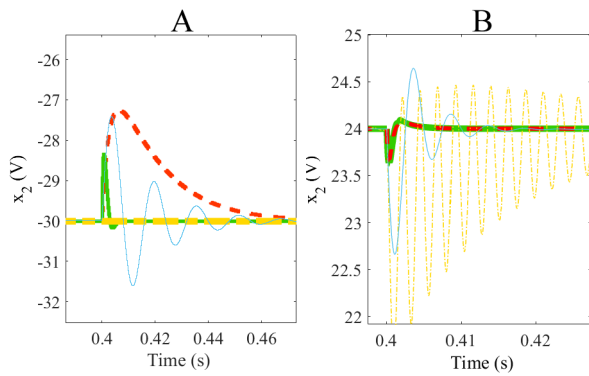


Fig. 6. Software simulation result (Matlab/Simulink) using control techniques SFL (dashed red), D-SFL (continue green) D-CICAPBC (continue cyan), D-IDAPBC (dashed yellow). Output voltage x_2 for buck-boost (A) and buck (B) in view of input variation (50 \rightarrow 30 V) in 0.4s.

even for the oscillatory dynamics. None of the implemented systems in software or in HIL presents instability. This attests that the embedded models and control equations are adequate to controlling the systems, and so, validating the control techniques. The processing time for the DSP (model Texas Instruments 28389D) to evaluate the control law and, consequently, to run a real-time simulation, is 1.2 μ s. Using a switching frequency $f_s = 50\text{kHz}$ ($T_s = 20\mu\text{s}$), the processing time of all control equations ($<1.5\mu\text{s}$) demands 6% of the bandwidth.

V. EXPERIMENTAL VALIDATION

The proposed control strategy was experimentally validated through a DC-DC converter prototype, Figure 12, development with kit BOOSTXL-3PHGANINV Evaluation Module of Texas Instruments [34]. The prototype consists of a three-phase GaN bridge module and a module of inductors and capacitors forming the passive elements of the buck and boost.

Figure 7 (PI) and Figure 8 (D-SFL) show the output voltage and the inductor current for a step variation of setpoint $x_{1d} = 1\text{A} \Rightarrow 3\text{A}$. The output reference voltage V_d is set initially to 4 V, at $t = 2\text{ms}$ it changes to 12 V and at $t = 14\text{ms}$ returns to 4 V. Figure 9 presents the details of experimental waveforms.

As it is shown in Figure 10 and Figure 11, during the first 10 ms, both PI and D-SFL controllers regulate the output voltage at the desired level after transient.

The regulator design is typically driven by specifications concerning the required closed loop speed of response or, equivalently, the maximum allowed tracking error with respect to the reference signal. These specifications can be turned into equivalent specifications for the closed loop bandwidth and phase margin [35]. In our case, the current controller, a closed loop bandwidth equal to about 1/5 of the switching frequency ($f_c = 20\text{kHz}$), to be achieved with, at least, a 60 degrees phase

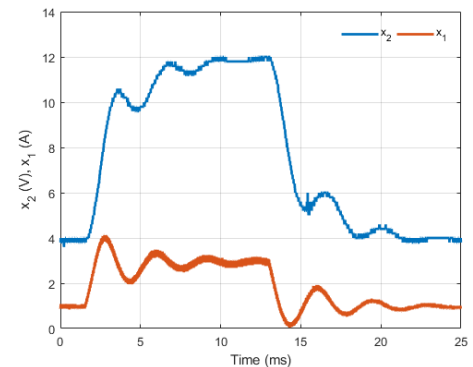


Fig. 7. Experimental result for buck - PI. Output voltage and inductor current - Setpoint variation.

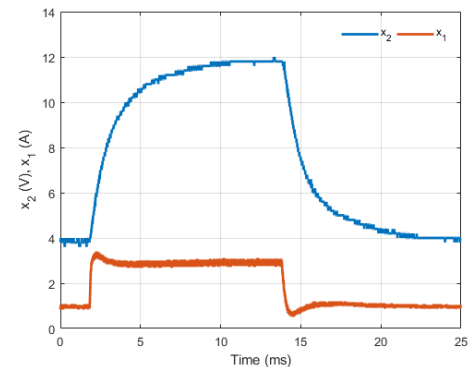


Fig. 8. Experimental result for buck - D-SFL. Output voltage and inductor current - Setpoint variation.

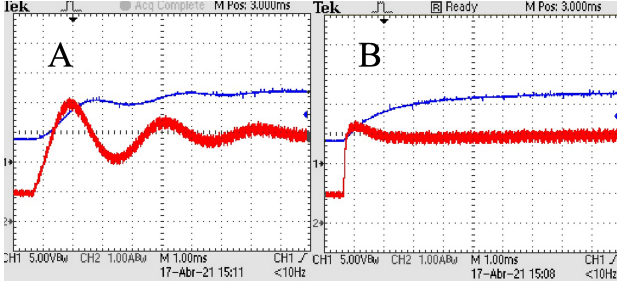


Fig. 9. Details of experimental results for buck - PI (A) and D-SFL (B). Output voltage (blue) and inductor current (red) - 12 V Setpoint.

TABLE VIII
Initial and converters parameters

Parameters	Buck-boost	Buck
x_{1d}	$\frac{G}{E} V_d^2$	GV_d
R	10 Ω	10 Ω
L	322 μH	322 μH
C	400 μF	400 μF
E	50 V	50 V
V_d	-30 V	25 V
f	50 kHz	50 kHz
k_1	3	3
k_z	-300	-500
k_{int}	-300	-300
k_α	0,77	0,77

TABLE IX
Experimental Buck

x_{1d}	$\frac{G}{E} V_d^2 = 1\text{A}$
R	4 Ω
L	322 μH
C	400 μF
E	24 V
V_d	12 V
f	20 kHz
k_1	6
k_{int}	5

margin.

In order to test the d-transform property of the controllers,

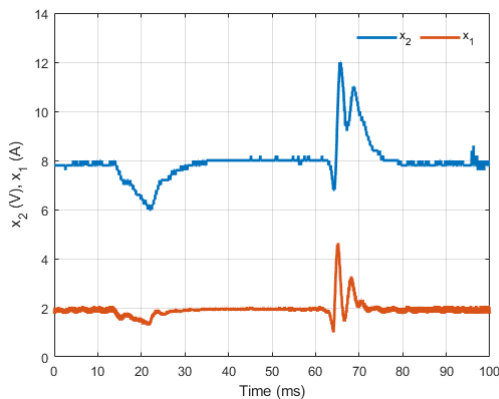


Fig. 10. Experimental result for buck - PI. Output voltage and inductor current with change of input voltage.

the value of input voltage E is changed ($24\text{V} \Rightarrow 12\text{V} \Rightarrow 24\text{V}$) as shown in Figure 10 and Figure 11. It is possible to verified that the D-SFL response presents less oscillations and smaller overshoot. Thus, the phase margin is greater for D-SFL compared with the classical PI.

VI. CONCLUSION

A new family of nonlinear controllers was proposed using the D-transform. In a new way, this method has a potentially useful properties for power converter applications. Based on the boost converter, control laws were generated for the buck and buck-boost converters (new d and new δ). Different alternatives were presented to show more than one way to find other candidates, which are proved to be stable control laws and eventually to present better performance.

The main contribution of this paper is to open new possibilities of stable nonlinear control laws for dc-dc converters, by a simple and direct methodology. It should be noted that the result obtained for the buck-boost - shown in Figs. 5-A and 6-A (yellow line)- is quite feasible and contains the following advantages:

- low overshoot under load and input variations;
- rapid response speed;
- does not require the measurement of the inductor current x_1 simplifying the controller design;
- low number of counts (compared with the work of [36]).

Future research will concentrate in generalized stability proof of the transformations and the application extension to SEPIC, CUK and Three-phase converters. Additionally, the inverse process of generating equations having the buck and buck-boost as base converters will be investigated.

ACKNOWLEDGEMENT

This work has been supported by the Brazilian agency CAPES.

Conflict of interest

None declared

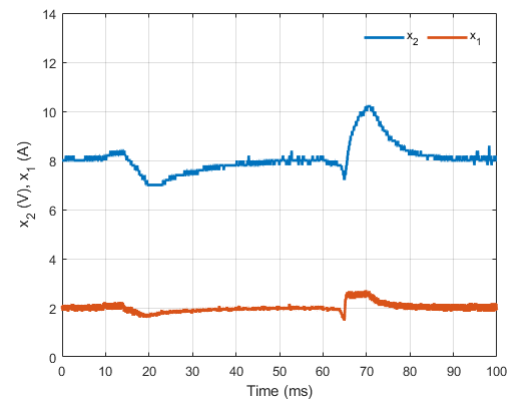


Fig. 11. Experimental result for buck - D-SFL. Output voltage and inductor current with change of input voltage.

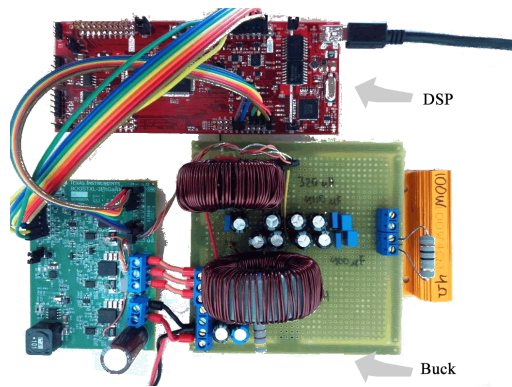


Fig. 12. DC-DC converter prototype

REFERENCES

- [1] G. Garcia, O. Lopez Santos, "A Unified Approach for the Control of Power Electronics Converters. Part I—Stabilization and Regulation", *Applied Sciences*, vol. 11, no. 2, p. 631, 2021.
- [2] S. K. Mazumder, A. Kulkarni, S. Sahoo, F. Blaabjerg, A. Mantooth, J. Balda, Y. Zhao, J. Ramos-Ruiz, P. Enjeti, P. Kumar, *et al.*, "A review of current research trends in power-electronic innovations in cyber-physical systems", *IEEE Journal of Emerging and Selected Topics in Power Electronics*, 2021.
- [3] Q. Xu, N. Vafamand, L. Chen, T. Dragičević, L. Xie, F. Blaabjerg, "Review on advanced control technologies for bidirectional dc/dc converters in dc microgrids", *IEEE Journal of Emerging and Selected Topics in Power Electronics*, 2020.
- [4] C. A. Albugeri, N. C. Dal Pont, T. K. Jappe, S. A. Mussa, T. B. Lazzarin, "Control system for multi-inverter parallel operation in uninterruptible power systems", *Eletrônica de Potência-SOBRAEP*, vol. 24, no. 1, pp. 37–46, 2019.
- [5] R. G. Cacau, T. B. Lazzarin, M. C. Villanueva, I. Barbi, "Study of High Step-Up Gain DC-DC Converters Based on Stacking of Non-Isolated Topologies", *Eletrônica de Potência-SOBRAEP*, vol. 23, no. 4, pp. 505–515, 2018.
- [6] H. Lee, V. Smet, R. Tummala, "A review of sic power module packaging technologies: Challenges, advances, and emerging issues", *IEEE Journal of Emerging and Selected Topics in Power Electronics*, vol. 8, no. 1, pp. 239–255, 2019.
- [7] J. Feng, W. Chu, Z. Zhang, Z. Zhu, "Power electronic transformer-based railway traction systems: Challenges and opportunities", *IEEE Journal of Emerging and Selected Topics in Power Electronics*, vol. 5, no. 3, pp. 1237–1253, 2017.
- [8] M. Elkazaz, M. Sumner, D. Thomas, "Energy management system for hybrid PV-wind-battery microgrid using convex programming, model predictive and rolling horizon predictive control with experimental validation", *International Journal of Electrical Power & Energy Systems*, vol. 115, p. 105483, 2020.
- [9] P. Ewald, R. V. Tambara, H. A. Gründling, "A direct discrete-time reduced order robust model reference adaptive control for grid-tied power converters with LCL filter.", *Revista Eletrônica de Potência*, vol. 25, no. 3, pp. 361–372, 2020.
- [10] M. A. Mohamed, H. M. Abdullah, M. A. El-Meligy, M. Sharaf, A. T. Soliman, A. Hajjiah, "A novel fuzzy cloud stochastic framework for energy management of renewable microgrids based on maximum deployment of electric vehicles", *International Journal of Electrical Power & Energy Systems*, vol. 129, p. 106845, 2021.
- [11] J. He, D. Zhang, D. Torrey, "Recent advances of power electronics applications in more electric aircrafts", in *2018 AIAA/IEEE Electric Aircraft Technologies Symposium (EATS)*, pp. 1–8, IEEE, 2018.
- [12] B. Zhou, Y. Meng, W. Huang, H. Wang, L. Deng, S. Huang, J. Wei, "Multi-energy net load forecasting for integrated local energy systems with heterogeneous prosumers", *International Journal of Electrical Power & Energy Systems*, vol. 126, p. 106542, 2021.
- [13] P. T. Krein, J. A. Galtieri, "Active Management of Photovoltaic System Variability with Power Electronics", *IEEE Journal of Emerging and Selected Topics in Power Electronics*, 2020.
- [14] G. V. Hollweg, P. J. Ewald, G. G. Koch, E. Mattos, R. V. Tambara, H. A. Gründling, "Controlador Robusto Adaptativo Super-Twisting Sliding Mode por Modelo de Referência para Regulação das Correntes Injetadas em Redes Fracas por Inversores Trifásicos com Filtro LCL", *Revista Eletrônica de Potência*, vol. 26, no. 2, pp. 1–12, 2021.
- [15] A. Rosa, L. Morais, G. Fortes, S. S. Júnior, "Practical considerations of nonlinear control techniques applied to static power converters: A survey and comparative study", *International Journal of Electrical Power & Energy Systems*, vol. 127, p. 106545, 2021.
- [16] J. F. Silva, S. F. Pinto, "Linear and nonlinear control of switching power converters", in *Power Electronics Handbook*, pp. 1141–1220, Elsevier, 2018.
- [17] F. Vatansever, N. Yalcin, "e-Signals&Systems: A web-based educational tool for signals and systems", *Computer Applications in Engineering Education*, vol. 25, no. 4, pp. 625–641, 2017.
- [18] O. Gehan, E. Pigeon, T. Menard, M. Pouliquen, H. Gualous, Y. Slamani, B. Tala-Ighil, "A nonlinear state feedback for DC/DC boost converters", *Journal of Dynamic Systems, Measurement, and Control*, vol. 139, no. 1, p. 011010, 2017.
- [19] S. Arora, P. Balsara, D. Bhatia, "Input-Output Linearization of a Boost Converter with Mixed Load (Constant Voltage Load and Constant Power Load)", *IEEE Transactions on Power Electronics*, vol. PP, no. 99, pp. 1–9, 2018.
- [20] M. Zhang, R. Ortega, Z. Liu, H. Su, "A new family of interconnection and damping assignment passivity-based controllers", *International Journal of Robust and Nonlinear Control*, vol. 27, no. 1, pp. 50–65, 2017.
- [21] V. V. Paduvali, R. Taylor, L. R. Hunt, P. Balsara, "Mitigation of Positive Zero Effect on Nonminimum Phase Boost DC–DC Converters in CCM", *IEEE*

Transactions on Industrial Electronics, vol. 65, no. 5, pp. 4125–4134, 2018.

- [22] Y. Zhang, J. Liu, Z. Dong, H. Wang, Y. Liu, “Dynamic performance improvement of diode–capacitor-based high step-up dc–dc converter through right-half-plane zero elimination”, *IEEE Transactions on Power Electronics*, vol. 32, no. 8, pp. 6532–6543, 2017.
- [23] H. J. Sira-Ramirez, R. Silva-Ortigoza, *Control design techniques in power electronics devices*, Springer Science & Business Media, 2006.
- [24] R. W. Erickson, D. Maksimovic, *Fundamentals of power electronics*, Springer Science & Business Media, 2007.
- [25] H. Rodriguez, R. Ortega, G. Escobar, “A new family of energy-based non-linear controllers for switched power converters”, in *Industrial Electronics, 2001. Proceedings. ISIE 2001. IEEE International Symposium on*, vol. 2, pp. 723–727, IEEE, 2001.
- [26] H. Sira-Ramirez, R. A. Perez-Moreno, R. Ortega, M. Garcia-Esteban, “Passivity-based controllers for the stabilization of DC-to-DC power converters”, *Automatica*, vol. 33, no. 4, pp. 499–513, 1997.
- [27] S. Sastry, *Nonlinear systems: analysis, stability, and control*, vol. 10, Springer Science & Business Media, 2013.
- [28] S. I. Seleme, L. M. F. Morais, A. H. R. R., L. A. B. Torres, “Stability in passivity-based boost converter controller for power factor correction”, *European Journal of Control*, vol. 19, no. 1, pp. 56–64, 2013.
- [29] C. Wang, D. Sun, W. Gu, “Stability Analysis of Constant Current Controlled Primary-Side Regulation Flyback Converter”, *IEEE Journal of Emerging and Selected Topics in Power Electronics*, 2020.
- [30] A. H. Rosa, L. M. Morais, T. M. de Souza, I. Seleme, “Comparison of nonlinear control techniques applied to SEPIC and CUK converters with reduced modeling and hybrid solutions”, in *2016 12th IEEE International Conference on Industry Applications (INDUSCON)*, pp. 1–8, IEEE, 2016.
- [31] P. Borja, E. Ortega, R. and Nuño, “New results on PID passivity-based controllers for port-Hamiltonian systems”, *IFAC-PapersOnLine*, vol. 51, no. 3, pp. 175–180, 2018.
- [32] M. Zhang, P. Borja, R. Ortega, Z. Liu, H. Su, “PID Passivity-Based Control of Port-Hamiltonian Systems”, *IEEE Transactions on Automatic Control*, vol. 63, no. 4, pp. 1032–1044, 2018.
- [33] A. Rosa, M. Silva, M. Campos, R. Santana, W. Rodrigues, L. Morais, S. Seleme Jr., “SHIL and DHIL Simulations of Nonlinear Control Methods Applied for Power Converters Using Embedded Systems”, *Electronics*, vol. 7, no. 10, p. 241, 2018.
- [34] Texas Instruments, “BOOSTXL-3PHGANINV 48-V Three-Phase Inverter With Shunt-Based In-Line Motor Phase Current Sensing Evaluation Module”, <https://www.ti.com/tool/BOOSTXL-3PHGANINV>, online; accessed 17 April 2021.
- [35] S. Buso, P. Mattavelli, “Digital control in power electronics”, *Synthesis Lectures on Power Electronics*, vol. 5, no. 1, pp. 1–229, 2015.

- [36] W. He, C. A. Soriano-Rangel, R. Ortega, A. Astolfi, F. Mancilla-David, S. Li, “Energy shaping control for buck–boost converters with unknown constant power load”, *Control Engineering Practice*, vol. 74, pp. 33–43, 2018.

BIOGRAPHIES

Arthur Hermano Rezende Rosa, Bachelor’s at Control and Automation Engineering (2007), master’s at Electric Engineering (2011) and PhD at Electric Engineering from Universidade Federal de Minas Gerais (2015). Has experience in Electric Engineering, focusing on Control of Electronic Processes, Feedback, acting on the following subjects: passivity, nonlinear control, power factor correction, adaptive control, dsp and applied control.

Waner Wodson Aparecido Gonçalves Silva, received the degree in electrical engineering from Faculdades Santo Agostinho in 2011, and the M.Sc. degree from the Federal University of Minas Gerais in 2013. He is currently an Assistant Professor with the Federal University of Itajuba, Campus Itabira, and lecturing classes on power electronics and embedded systems. His research interests include power electronic applications in renewable energy, energy storage, and embedded systems.

Wei He is with the School of Automation, Nanjing University of Information Science and Technology, China. His research interests include control of power electronics and nonlinear control.

Fernando Andrade da Silva, is a Control and Automation Engineer graduated from the Federal Institute of Minas Gerais. Currently working as an Engineering Analyst, working on innovation projects, development and implementation of solutions for the mineral sector. He has experience in the field of instrumentation, studies and specification of equipment/instruments for process control.

Lenin Martins Ferreira Morais, (Member, IEEE) received the B.Sc., M.Sc., and Ph.D. degrees in electrical engineering from the Federal University of Minas Gerais (UFMG), Belo Horizonte, Brazil, in 2000, 2002, and 2007, respectively. He completed a Postdoctoral Internship in Laboratoire Laplace, Toulouse, France, He is currently an Associate Professor with the Federal University of Minas Gerais, Belo Horizonte, Brazil, has experience in electrical engineering, with emphasis in industrial electronics, systems and electronic controls, working mainly in the subjects, including power electronics, high efficiency converters, LEDs drivers, PFC converters, PWM techniques, and solid-state transformer.

Seleme Isaac Seleme Jr, received the B.S. degree in electrical engineering from the Escola Politecnica (USP), São Paulo, Brazil, in 1977, the M.S. degree in electrical engineering from the Federal University of Santa Catarina, Florianópolis, Brazil, in 1985, and the Ph.D. degree in control and automation from the Institut National Polytechnique de Grenoble, France, in 1994. He is currently a Full Professor with the Department of Electronic Engineering, Federal University of Minas Gerais, Belo Horizonte, Brazil. His main research interests include renewable energy systems, modular multilevel converters, and nonlinear control applied to power converters.